https://doi.org/10.22226/2410-3535-2021-4-462-466 PACS: 81.05.-t; 81.15.Cd

Effect of copper concentrations on microstructure, residual stress and corrosion behavior of Ni_{100-x}-Cu_x alloy films processed by magnetron co-sputtering

Mukesh Kumar

Department of Physics, Faculty of Science, Shree Guru Govind Singh Tricentenary University, Gurgaon, Delhi-NCR, 122001, India

mukesh.kumar@sgtuniversity.org

Nickel based alloys have gained importance due to their very good mechanical properties as well as their electrochemical behavior in different environmental conditions. In this regard, thin films of nanocrystalline Ni-Cu alloys have been processed by RF/DC magnetron co-sputtering in Ar gas environment for different copper concentration (10%, 21%, 28% and 39%). Grain size determination, phase identification and residual stress measurement have been done using an X-ray diffraction technique. A compressive residual stress has been observed and the value of the compressive stress increases with an increase in the Cu concentration in the Ni_{100-x}-Cu_x alloy films. The electrochemical behavior of thin films of the Ni_{100-x}-Cu_x alloy has been investigated with the help of potentiodynamic polarization experiments which revealed susceptibility towards pitting corrosion. The rate of corrosion decreases from 0.92×10^{-2} to 0.26×10^{-2} mm/year with the increase in Cu concentration from 10% to 39%. The microstructure of thin films of the Ni_{100-x}-Cu_x alloy has been investigated using a field emission scanning electron microscope (FESEM). The FESEM micrograph shows the formation of pits, and the size of pits decreases with increasing concentration of doped Cu. Experimental results also reveal that the increase in corrosion resistance can correlate with the developing residual stress in the films.

Keywords: magnetron sputtering, Ni_{100-x}-Cu_x alloy films, microstructures, electrochemical behavior.

УДК: 538.9

Влияние концентрации меди на микроструктуру, остаточные напряжения и коррозионные свойства пленок сплава Ni_{100-x}-Cu_x, полученных методом совместного магнетронного распыления

Мукеш Кумар

Кафедра физики, факультет естественных наук, Университет трехсотлетия Шри Гуру Говинд Сингха, Гургаон, Дели, 122001, Индия

Сплавы на основе никеля приобрели важное значение из-за их очень хороших механических свойств, а также их электрохимического поведения в различных условиях окружающей среды. В связи с этим, тонкие пленки нанокристаллических сплавов Ni-Cu были получены RF/DC магнетронным распылением в среде газа Ar для различной концентрации меди (10%, 21%, 28% и 39%). Определение размера зерен, идентификация фаз и измерение остаточного напряжения проводились с использованием метода дифракции рентгеновских лучей. Наблюдается остаточное напряжение сжатия, и величина напряжения сжатия увеличивается с увеличением концентрации Cu в пленках сплава Ni_{100-x}-Cu_x. Электрохимическое поведение тонких пленок сплава Ni_{100-x}-Cu_x было исследовано с помощью экспериментов по потенциодинамической поляризации, которые выявили подверженность питтинговой коррозии. Скорость коррозии снижается с 0.92×10^{-2} до 0.26×10^{-2} мм/год при увеличении концентрации

Cu с 10% до 39%. Микроструктура тонких пленок сплава Ni_{100-x}-Cu_x была исследована с помощью автоэмиссионного сканирующего электронного микроскопа (FESEM). Микрофотография FESEM показывает образование ямок, размер ямок уменьшается с увеличением концентрации легированной меди. Экспериментальные результаты также показывают, что повышение коррозионной стойкости может коррелировать с развивающимся остаточным напряжением в пленках.

Ключевые слова: магнетронное распыление, пленки сплава Ni_{100-x}-Cu_x, микроструктуры, электрохимическое поведение.

1. Introduction

Films of Ni-based alloys have got significance worldwide due to their very good mechanical properties and greater resistance to corrosion in different environments. Particularly Ni-Cu alloy coatings have gained importance as a result of their better corrosion and mechanical properties along with magnetic and optical properties. Hence, Ni-based alloy coatings can be used as anticorrosive and hard coatings [1–7]. Ni-Cu alloy coatings have got potential application in metallurgical industry, in seawater applications, where high corrosion resistance is required [8–11].

There are several methods for processing nanocrystalline alloys such as vapor deposition, magnetron sputtering, electrode-deposition, and mechanical alloying [12–17]. A Ni-Cu alloy prepared by electrode deposition or mechanical alloying consists of many micro-pores, and micro-strain gives more preference for the corrosion attack. However, the magnetron sputtering technique assures more purity and higher density for the processed alloy films as compared to other mentioned techniques. In addition to that, the microstructural features of the processed films can be easily monitored using parameters associated with magnetron sputtering, such as substrate temperature, target power, gas pressure, and substrate bias [18–20]. So far, Ni-Cu alloy films have been mainly prepared via electrode deposition and investigated for application in MEMS devices or thermoelectric devices [11, 21, 22]. Ghosh et al. [13] prepared Ni-Cu alloy films by electrode deposition and studied their pitting corrosion behavior. Goronova et al. [23] processed Ni-Cu alloy films by the electrodeposition technique and characterized them for their suitable applications. Further, Deo et al. [24] studied electrodeposited Ni-Cu alloy films on a steel substrate for better corrosion properties. The main purpose of this investigation is to get films of the Ni-Cu alloy, deposited by magnetron sputtering, with varying copper concentrations along with the desired microstructure and grain size for their better electrochemical properties.

2. Experimental procedure

2.1. Processing

A magnetron sputtering system (model KVS-T 4065) was used for the processing of $Ni_{100-x}Cu_x$ alloy films. This system was equipped with two DC power sources associated with Ni and Cu targets. A base pressure lower than 2×10^{-6} Torr was achieved with the help of a rotary pump and a turbo-molecular pump before the start of sputtering. The investigated films were deposited on p-type Si (100) substrates which was ultrasonically cleaned with acetone and isopropanol. During deposition, the substrates were rotated at 25 rpm to obtain the compositional uniformity. The used deposition parameters, related to magnetron sputtering, are shown in Table 1.

2.2. Characterization

A surface profilometer (Dektak 150, USA) has been used to measure the thicknesses of the processed $Ni_{100-x}Cu_x$ films. Grazing incidence X-ray diffraction (GIXRD) (Philips X'Pert PRO Diffractometer) has been used to measure grain sizes and identify the phases present. The GIXRD was operated at an accelerating voltage of 40 K and a current of 30 mA using Cu-K_α radiation with a scanning speed of 0.05°/s in the range between 35° and 65°. For microstructural and elemental analysis, a field emission scanning electron microscope (FESEM) (Zeiss SUPRA 40, Germany) equipped with an energy dispersive X-ray (EDX) microanalyzer have been used. Autolab PG Stat-30 (Petentiostat/Galvanostat) has been used to analyze electrochemical behaviour. All electrochemical tests were performed in a 3.5% NaCl solution with pH ≈ 6.7 at room temperature. The silver/silver chloride electrode (Ag/AgCl) has been used as reference electrode with a platinum wire as a counter electrode, and the sample as a working electrode (area: 1 cm^2) for the present investigation. Further correlation of microstructure, grain size and Cu concentration of the processed Ni-Cu alloy films with their electrochemical behavior have been done.

Table 1. Parameters related to magnetron sputtering.

Processing parameters	Values
Base Pressure	2.0×10^{-6} Torr
Working Pressure	30 mTorr
Ar Gas Flow Rate	50 sccm
Ni DC Target Power	50 W
Cu DC Target Power	9 W, 12 W, 15 W, 18 W
Substrate Temperature	100°C
Negative Substrate Biasing	−60 V
Substrate Rotation Speed	25 rpm
Distance between Target and Substrate	150 mm

3. Results and discussion

3.1. Chemical composition

The compositions of the $Ni_{100-x}Cu_x$ alloy films determined by EDX analysis are x = 10, 21, 28, and 39. These average values of x are obtained by EDX analysis at five different places within the microstructure. Overall compositions of the processed $Ni_{100-x}Cu_x$ alloy films have been further confirmed with the ratios of individual growth rates of Ni and Cu films deposited using pure Ni and Cu targets, respectively.

3.2. X-ray diffraction analysis

The XRD patterns obtained for the $Ni_{100-x}Cu_x$ alloy films deposited at a substrate temperature of 100°C and a substrate bias of −60 V with a varying Cu target power is shown in Fig. 1. With the help of XRD peak widths, the calculated crystallite sizes using the Williamson-Hall method [25] are presented in Table 2. The values of crystallite sizes are found to decrease marginally, while micro-strain increases significantly with Cu doping. Using the $\sin^2\psi$ technique, the measured values of the principal normal residual stresses (σ_1 and σ_2) developed in the films of the $Ni_{100-x}Cu_x$ alloy are presented in Table 2.

These data show that the stress becomes more compressive when Ni is alloyed with Cu in the $Ni_{100-x}Cu_x$ alloy films. The compressive nature of the observed residual stress may be due to the difference in the size of Cu and Ni atoms, which leads to a change in the lattice parameter and, hence, in the volume of the unit cell. In addition to this, shot-peening produced by bombardment of neutral atoms on the growing film surfaces during the sputtering process can also lead to the development of the compressive stress. The higher root mean square (RMS) strain on alloying with Cu could be attributed to an increase in the amount of average variation of the atomic position from their original positions in the Ni lattice due to the higher atomic radius of the former type of atoms. This trend may be attributed to the lower growth rates of the $Ni_{100-x}Cu_x$ alloy films compared to that of pure Ni.

3.3. Microstructure

The representative microstructures of Ni, and $Ni_{100-x}Cu_x$ alloy films deposited at a negative substrate bias of −60 V and a substrate temperature of 100°C are shown in Fig. 2 a, b, c and d, respectively. The microstructure of pure Ni films appears to be courser and large clusters are formed (Fig. 2 a), whereas qualitative examination of the microstructures of the investigated $Ni_{100-x}Cu_x$ alloy films reveals the formation of finer and denser granular structures (Fig. 2 b, c and d) as compared to pure Ni films.

3.4. Corrosion behavior

The potentiodynamic polarization curves obtained for the nanocrystalline Ni and $Ni_{100-x}Cu_x$ alloy films subjected to corrosion tests in a 3.5 g/l NaCl solution are shown in Fig. 3. The corrosion potential (E_{corr}) and corrosion current density (I_{corr}) can be extracted from the intersection of the slopes of the potentiodynamic linear polarization using the Stern-Geary relation [26, 27]. Further, the corrosion rate can be calculated by using the following equation [27]:

$$\text{Corrosion rate} = I_{corr} \cdot M \cdot C / D \cdot V_l,$$

where M is the atomic mass, D is the density of the sample, V_l is the valence and C is a constant (≈3270) [27]. The obtained electrochemical parameters from the corrosion test are presented in Table 3.

The obtained results, presented in Table 3, show that the corrosion rates in a 3.5 g/l NaCl solution decreases, and the polarization resistance (R_p) increases with an increase in the Cu concentration in the films of the $Ni_{100-x}Cu_x$ alloy. This indicates that the corrosion resistance of pure Ni is improved by alloying with Cu.

The corroded surfaces of films of Ni and the $Ni_{100-x}Cu_x$ alloy have been examined using FESEM along with EDX analyses to understand the mechanism of degradation. The

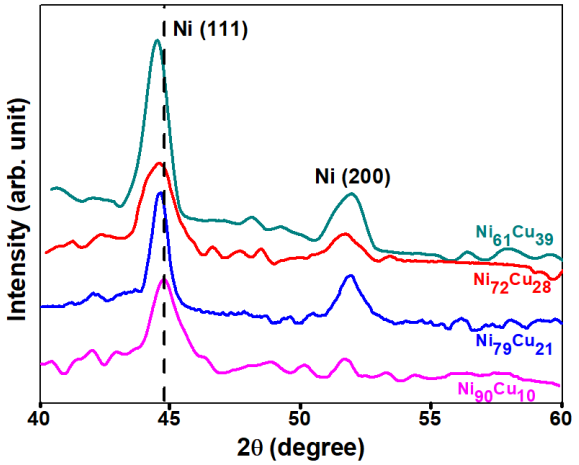

Fig. 1. (Color online) XRD patterns of Ni-Cu alloy films with varying Cu concentration.

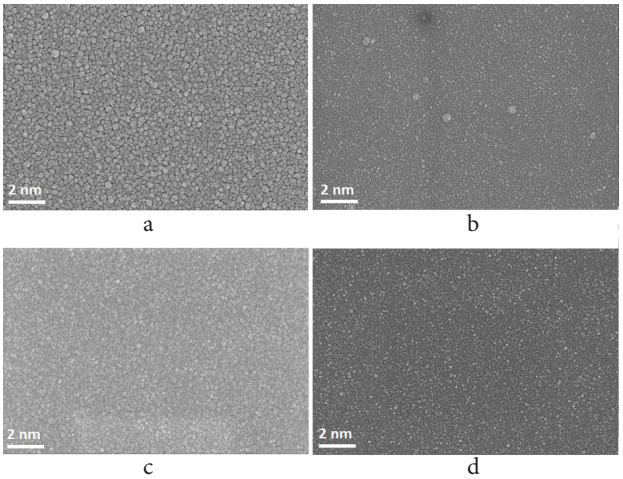

Fig. 2. Microstructure of: Ni (a), $Ni_{90}Cu_{10}$ (b), $Ni_{89}Cu_{21}$ (c), and $Ni_{61}Cu_{39}$ (d) alloy films processed at the parameters given in Table 1.

Table 2. Root mean square (RMS) strain, crystallite size and average biaxial residual stress obtained for the $Ni_{100-x}Cu_x$ alloy films.

	Root mean square (RMS) strain (×10⁻³)	Crystallite size (nm)	Residual stress (GPa)	
			Along x-axis (σ_1)	Along y-axis (σ_2)
$Ni_{90}Cu_{10}$	0.7	12.6 ± 0.3	−0.12 ± 0.2	−0.08 ± 0.1
$Ni_{79}Cu_{21}$	1.2	12.2 ± 0.4	−0.18 ± 0.3	−0.13 ± 0.2
$Ni_{72}Cu_{28}$	2.3	11.8 ± 0.2	−0.36 ± 0.3	−0.19 ± 0.2
$Ni_{61}Cu_{39}$	2.9	11.2 ± 0.3	−0.52 ± 0.4	−0.32 ± 0.3

Table 3. Electrochemical parameters of the $Ni_{100-x}Cu_x$ alloy films with varying copper concentration.

Cu concentration (%)	E_{corr} (V)	I_{corr} (A/cm^2)×10^{-6}	Polarization resistance, R_p (Ω)×10^3	Corrosion rate (mm/year) ×10^{-2})
0	−0.230	1.55	1.01	1.67
10	−0.206	1.05	4.7	0.92
21	−0.170	0.63	10.5	0.65
28	−0.156	0.55	12.4	0.43
39	−0.109	0.42	15.7	0.26

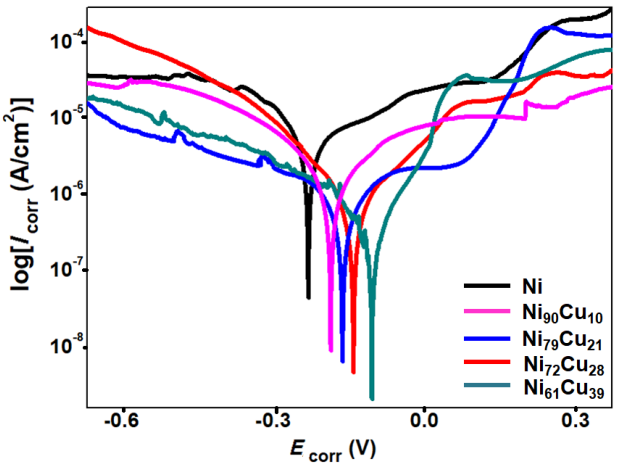

Fig. 3. (Color online) Potentiodynamic polarization curves of nanocrystalline Ni, and $Ni_{100-x}Cu_x$ alloy films in a 3.5 g/l NaCl solution.

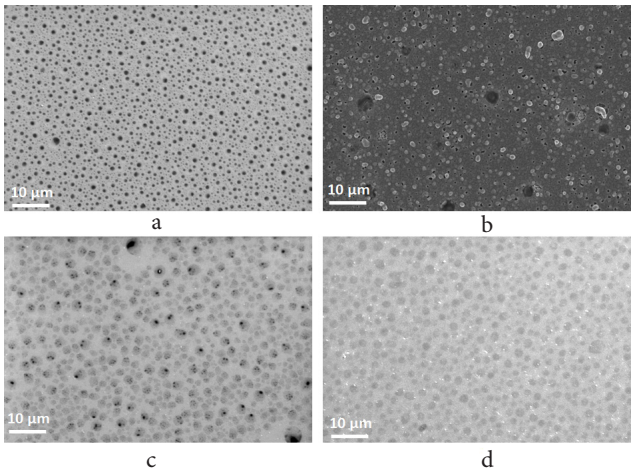

Fig. 4. Micrographs of the corroded surfaces of: Ni (a), $Ni_{90}Cu_{10}$ (b), $Ni_{89}Cu_{21}$ (c), and $Ni_{61}Cu_{39}$ (d) alloy films.

FESEM micrographs of the corroded surfaces of presently investigated thin films subjected to potentiodynamic polarization tests are shown in Fig. 4. on the investigation of the FESEM micrographs in Fig. 3 a and b shows that the corroded surfaces of nanocrystalline Ni and $Ni_{90}Cu_{10}$ films contain a high density of large pits, whereas the images representing the $Ni_{61}Cu_{39}$ (Fig. 4 d) alloy thin films do not show pits. Of course, the surface of the $Ni_{90}Cu_{10}$ (Fig. 4 b) and $Ni_{79}Cu_{21}$ (Fig. 4 d) alloy films show relatively fewer pits compared to that observed on the Ni surface (Fig. 4 a). The EDX analysis of the corroded surfaces being investigated in this study has shown evidence of significant enrichment of O, as shown in Fig. 5.

The increase in the Cu concentration in the $Ni_{100-x}Cu_x$ alloy films leads to the formation of more passive layers of Cu_2O [13], which protects the surface from corrosion. The activation of pitting corrosion in the $Ni_{100-x}Cu_x$ alloy films related to the selective dissolution of Ni, leading to the enrichment of C, at the expense of Ni inside the pits [28]. It has also been reported that the presence of Cl^- anions increases the potential difference across the developed passive film of Cu_2O on the surface, which leads to an increase in the diffusion rate of Ni^+ ion from the Ni-film interface to the film-solution interface, thus creating cation vacancies at the interface [13]. Therefore, for the higher concentration of Cl^-, it is expected to have more voids at the Ni-film interface. The growth of such voids leads to the formation of pits with selective dissolution of Ni along with the localized collapse of the formed passive film [29,30]. However, in the $Ni_{100-x}Cu_x$ alloy films, the resistance to pitting corrosion is observed to be enhanced with an increase in the Cu concentration due to formation of a passive layer of Cu_2O on the surface.

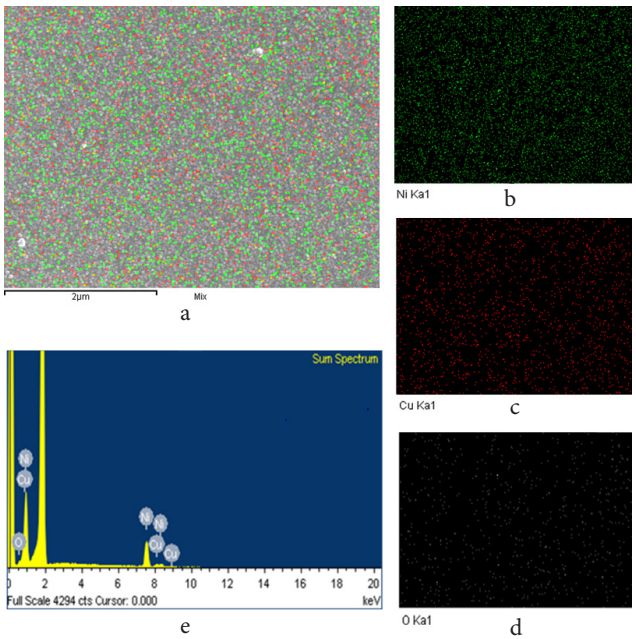

Fig. 5. (Color online) Corroded surface of $Ni_{90}Cu_{10}$ alloy films FESEM (SE) image (a), and corresponding EDX maps of: Ni (b), Cu (c), and O (d), as well as EDX spectrum (e).

4. Conclusions

Pure Ni film and $Ni_{100-x}Cu_x$ alloy films have been successfully processed by the magnetron co-sputtering technique with varying copper concentrations. The morphology of the dense surface and the variation in the grain size in the range of 11 to 12 nm has been observed for the investigated alloy

films. The processed nanocrystalline $Ni_{100-x}Cu_x$ alloy films have been found to possess compressive residual stress and the value of compressive stress increases with increasing Cu concentration. Nanocrystalline pure Ni as well as $Ni_{100-x}Cu_x$ alloy films are observed to be susceptible to pitting corrosion in a 3.5 g/l NaCl solution. Significant improvement in corrosion resistance has been observed in the $Ni_{100-x}Cu_x$ alloy films as compared to pure Ni films. The corrosion rate of the $Ni_{61}Cu_{39}$ alloy films is found to be (0.26×10^{-2} mm/year), which is the lowest among all other processed alloy films.

Acknowledgement. Author is thankful to SGT University, Gurugram and IIT Kharagpur, India for their supports.

References

1. M. Metikos-Hukovica, I. Skugorb, Z. Grubacb, R. Babic. Electrochim. Acta. 55, 3123 (2010). Crossref
2. A. A. Khadom, A. S. Yaro. Russ. J. Phys. Chem. A. 85, 2005 (2011). Crossref
3. S. Mukherjee, A. K. Ghosh. Mater. Sci. Eng. A. 528, 3289 (2011). Crossref
4. A. A. Khadom, A. S. Yaro, A. Y. Musa, A. B. Mohamad, A. H. Kadhum. J. Korean Chem. Soc. 56, 406 (2012). Crossref
5. S. Bhattacharya, G. P. Dinda, A. K. Dasgupta, H. Natu, B. Dutta, J. Mazumder. J. Alloys Compd. 509, 6364 (2011). Crossref
6. E. Pellicer, A. Varea, S. Pané, K. M. Sivaraman, B. J. Nelson, S. Suriñach, M. D. Baró, J. Sort. Surf. Coat. Technol. 205, 5285 (2011). Crossref
7. A. Varea, E. Pellicer, S. Pané, B. J. Nelson, S. Suriñach, M. D. Baró, J. Sort. Int. J. Electrochem. Sci. 7, 1288 (2012).
8. I. Baskaran, T. S. N. Sankara Narayanan, A. Stephen. Mater. Lett. 60, 1990 (2006). Crossref
9. M. Alper, H. Kockar, M. Safak, M. C. Baykul. J. Alloys Compd. 453, 15 (2008). Crossref
10. Q. Do, H. An, G. Meng, W. Li, L. Zhang, Y. Wang, B. Liu, J. Wang, F. Wang. J. Mater. Sci. Technol. 35, 2144 (2019). Crossref
11. M. S. Safavi, M. Fathi, S. Mirzazadeh, A. Ansarian, I. Ahadzadeh. Surface Engineering. 37, 226 (2021). Crossref
12. M. Kumar. Letters on Materials. 11 (3), 315 (2021). Crossref
13. S. K. Ghosh, A. K. Grover, G. K. Dey, M. K. Totlani. Surf. Coat. Technol. 126, 48 (2000). Crossref
14. S. Konovalov, K. Osintsev, A. Golubeva, V. Smelov, Y. Ivanov, X. Chen, I. Komissarova. Journal of Materials Research and Technology. 9 (4), 8796 (2020). Crossref
15. S. Qian, Y. Dai, Y. Guo, Y. Zhang. Materials. 14 (4), 781 (2021). Crossref
16. X. Yang, Y. Yagodzinskyy, Y. Ge, E. Lu, J. Lehtonen, L. Kollo, S. P. Hannula. Metals. 11 (6), 872 (2021). Crossref
17. L. Liu, Y. Li, F. Wang. Electrochim. Acta. 52, 7193 (2007). Crossref
18. M. Kumar, R. Mitra. Thin Solid Films. 624, 70 (2017). Crossref
19. M. Kumar, R. Mitra. Surf.Coat.Technol. 251, 239 (2014). Crossref
20. M. Kumar, S. Mishra, R. Mitra. Surf.Coat.Technol. 228, 100 (2013). Crossref
21. S. G. Hur, D. J. Kim, B. D. Kang, S. G. Yoon. J. Vac. Sci. Technol., B. 22, 2698 (2004). Crossref
22. Y. W. Huang, T. Y. Chao, C. C. Chen, Y. T. Cheng. Appl. Phys. Lett. 90, 244105 (2007). Crossref
23. D. Goranova, G. Avdeev, R. Rashkov. Surface & Coatings Technology. 240, 204 (2014). Crossref
24. Y. Deo, S. Guha, K. Sarkar, P. Mohanta, D. Pradhan, A. Mondal. Applied Surface Science. 515, 146078 (2020). Crossref
25. G. K. Williamson, W. H. Hall. Acta Metall. 1, 22 (1953). Crossref
26. M. Stern, A. L. Geary. J. Electro. Soci. 104, 56 (1957). Crossref
27. M. Stern. Corrosion. 14, 440 (1958).
28. E. M. Sherif, A. A. Almajid, A. K. Bairamov, E. Al-Zahrani. Int. J. Electrochem. Sci. 6, 5430 (2011).
29. J. A. Ali, J. R. Ambrose. Corrosion Science. 33, 1147 (1992). Crossref
30. K. Banerjee, U. K. Chatterjee. Scripta Met. 44, 213 (2001). Crossref